Article

Optimization of Biodiesel Production Using Nanomagnetic CaO-Based Catalysts with Subcritical Methanol Transesterification of Rubber Seed Oil

Veronica Winoto [ORCID] **and Nuttawan Yoswathana** *

Department of Chemical Engineering, Faculty of Engineering, Mahidol University, Nakhon Pathom 73170, Thailand; vwinoto168@gmail.com or veronica.win@student.mahidol.edu

* Correspondence: egnyw8846@gmail.com or nuttawan.yos@mahidol.edu; Tel.: +662-889-2138 (ext. 6101)

check for
updates

Abstract: The molar ratio of methanol to rubber seed oil (RSO), catalyst loading, and the reaction time of RSO biodiesel production were optimized in this work. The response surface methodology, using the Box–Behnken design, was analyzed to determine the optimum fatty acid methyl ester (FAME) yield. The performance of various nanomagnetic CaO-based catalysts—KF/CaO-Fe_3O_4, KF/CaO-Fe_3O_4-Li (Li additives), and KF/CaO-Fe_3O_4-Al (Al additives)—were compared. Rubber seed biodiesel was produced via the transesterification process under subcritical methanol conditions with nanomagnetic catalysts. The experimental results indicated that the KF/CaO-Fe_3O_4-Al nanomagnetic catalyst produced the highest FAME yield of 86.79%. The optimum conditions were a 28:1 molar ratio of methanol to RSO, 1.5 wt % catalyst, and 49 min reaction time. Al additives of KF/CaO-Fe_3O_4 nanomagnetic catalyst enhanced FAME yield without Al up to 18.17% and shortened the reaction time by up to 11 min.

Keywords: rubber seed oil; biodiesel production; nanomagnetic catalyst; subcritical methanol; FAME yield; Box-Behnken design

1. Introduction

The International Energy Agency (IEA) has reported that the global energy demand in 2020 would be 14,896 million tons of oil equivalent (Mtoe) and up to 18,048 Mtoe by 2035. The finite supply and depletion of fossil energy reserves, coupled with increased energy consumption is placing higher demands on energy production [1]. Renewable energy technology was introduced as an alternative energy to fulfill these needs. However, renewable energy contributes only 20% to the global energy demand and the other 80% is still supplied by fossil fuels [2]. Therefore, further studying and improving production technology is required [3]. Biodiesel—a liquid fuel produced from edible or non-edible vegetable oil or animal fats [4]—is an environmental friendly alternative energy, renewable, energy efficient, substitution fuel that does not sacrifice an engine's operational performance [5]. The increasing demand for biodiesel is also due to awareness of the environmental impact of emissions from conventional fossil fuel combustion and the decline in domestic oil production [6].

Rubber seed, the agriculture residues considered as waste in the rubber industry, has the potential to be a non-edible biodiesel production source in many country, such as Thailand [7], Malaysia [8], Indonesia [9], and Bangladesh [10]. The oil content in rubber seed is high, between 40 and 50% [11], so it has attracted attention as a biodiesel raw material. Thailand is an agricultural country and the largest rubber producer, producing 35% of the world's total production [12], with the rubber tree plantations covering around 3,548,274 ha or 35,482.7 km^2. This amount is continuously increasing each year [13].

For the conventional biodiesel technique, transesterification with methyl ester is performed with a homogeneous catalyst such as potassium methoxide or potassium hydroxide [14,15]. The catalysts have high activity and conversion ability, but they produce a large amount of chemical waste water [16], long-term consuming production, are expensive, and catalyst removal or recovery are difficult [14]. Therefore, heterogeneous catalysts were studied to replace homogeneous catalysts. Presently, heterogeneous nanocatalysts have exhibited good catalyst properties: high activity and large surface area. Most recent studies have shown that they demonstrated better performance and are more effective, easy to handle, and cost efficient [16]. CaO-based catalysts are widely used for biodiesel production due to their high efficiency in FAME enhancement, low cost, and availability [17,18]. For example, heterogeneous catalysts with CaO-based catalysts such as CaMgO, CaZnO [19], CaO-NiO, CaO-Nd_2O_3 [20], and CaO-La_2O_3 [21] improved biodiesel production and the resultant yields were 83%, 81% [19], 86.3%, 82.2% [20], and 86.5% [21], respectively. After combining the magnetic catalysts and nanocatalysts together, nanomagnetic catalysts were formed. The nanomagnetic catalyst has good catalyst properties conferred by the nanocatalyst and is easily removed due to its magnetic properties [14]. The heterogeneous CaO-based catalysts with Li additives reduced soaps formation due to the reaction of alkaline catalysts with free fatty acids or the saponification of triglycerides and enhanced methyl esters [22,23]. Similarly, the presence of Al additives in the form of sodium meta-aluminate improved transesterification in biodiesel production. Hence, both additives enhanced methyl esters production. The Al additives in CaO-based catalysts improved catalyst performance along with the presence of Na, an alkali metal that behaves similarly to Li [24].

The subcritical fluid technique was developed as a novel technique for biodiesel production. It is mostly considered environmental friendly and inexpensive due to the significant in of the production time [25]. The main advantages of transesterification in subcritical condition for biodiesel production was high conversion and reaction rates [26]. The operating temperature under subcritical methanol ranges from 150 to 250 °C [26,27]. Subcritical methanol at 220 °C achieved the highest FAME yield. For example, a 95.6% yield was obtained from soybean oil with K_3PO_4 [28], 94.7% from *Castor* oil, and 95.6% [29] from soybean oil with Na_2SiO_3 [30]. In the subcritical state, hydrogen bonding significantly decreases, which allows methanol to be a free monomer. The transesterification is completed via a methoxide transfer, whereby the fatty acid methyl ester and diglycerides are formed. Similarly, diglyceride is transesterified to form methyl ester and monoglycerides, which are further converted to methyl ester and glycerol in the last step [31].

Response Surface Methodology (RSM) with Box-Behnken experimental design have been effectively applied to determined optimum conditions. Mathematical and statistical methods have been used to predict the effect of input process parameters based on the output responses [32–34]. The three parameters that most influence biodiesel production are: methanol/oil ratio, catalyst loading, and reaction time [35,36].

In this research, rubber seed oil (RSO) was selected as a potential non-edible raw material for biodiesel production. Nanomagnetic catalysts were synthesized and applied in subcritical methanol biodiesel production to enhance biodiesel yield. The Box-Behnken experimental design, the most widely used for response surface methodology [37,38], was used to study the effect of each individual variable, such as molar ratio between methanol and RSO, catalyst amount, and reaction time. The response surface results were analyzed based on FAME yield percentage to determine the optimum conditions for rubber seed biodiesel production using subcritical methanol with nanomagnetic catalysts.

2. Materials and Methods

2.1. Materials

We used RSO and methanol (AR Grade, RCI Labscan, Bangkok, Thailand) as the raw materials for biodiesel production. The magnetic core (Fe_3O_4) was prepared from $FeSO_4 \cdot 7H_2O$ (AR Grade,

Ajax Finechem Pty Ltd., Victoria, Australia), Fe(SO$_4$)$_3$ (AR Grade, Ajax Finechem Pty Ltd.), and NH$_3$·H$_2$O (25% ACS Reagent, J.T. Baker, Pittsburgh, PA, USA). The metal oxide base that was chosen was CaO (AR Grade, Ajax Finechem Pty Ltd.). In the impregnation method, calcined metal oxides mixed with a magnetic core were dipped in KF (AR Grade, Ajax Finechem Pty Ltd.). For Li and Al additives catalysts, LiNO$_3$ (AR Grade, Ajax Finechem Pty Ltd.) and Al with NaOH (AR Grade, Ajax Finechem Pty Ltd.), which formed sodium meta-aluminate, were added in nanomagnetic CaO-based catalysts.

2.2. Preparation of Rubber Seed Oil

Rubber seeds were planted and harvested in Phattalung, a southern province in Thailand. The RSO was obtained from Agricultural Occupation Promotion and Development Center in Cha-am district, Phetchaburi province, Thailand. Firstly, rubber seeds were inserted to the deshelling machine. Then, the deshelled rubber seeds were dried at 60 °C for 4 h before the extraction process. The mechanical hydraulic pressing machine was used to crush and squeeze the rubber seeds to obtain rubber seed oil. The oil was then analyzed using the ASTM D5555-95 (2011) standard test method [32]. The initial free fatty acids (FFA) content of rubber seed oil was 16.72%.

2.3. Preparation of Nanomagnetic Catalysts

The nanomagnetic catalyst preparation procedures were modified based on the literature [16,22–24]. Firstly, the magnetic core was prepared by dissolving 27.8 g FeSO$_4$·7H$_2$O and 79.6 g Fe$_2$(SO$_4$)$_3$ 79.6 g in deionized water. Then, 25% NH$_3$·H$_2$O was added dropwise to the iron mixed solution. The mixed solution was vigorously stirred in a 60 °C water bath for 60 min. The final pH value of the aqueous solution was maintained at approximately 12.0. The mixed solution was then aged for 60 min. After aging, the black solid part that settled was then separated using a permanent magnet. The separated black solid was washed with distilled water until the final pH of the filtrate remained at 7.0. the wet magnetic core was dried at 60 °C for 24 h. After that, the black dried solid was pulverized into a fine black magnetic core powder. The metal oxide, CaO, was calcined at 600 °C for 3 h before the nanomagnetic solid base catalyst was prepared. Then, 100.0 g calcined metal oxides and a 5.0 g Fe$_3$O$_4$ magnetic core were mixed homogeneously. The impregnation method was performed next by completely dipping the mixture in 25 wt % KF aqueous solution, and then dried at 105 °C for 24 h. The dried mixture was calcined in a furnace at 600 °C [16]. As such, the synthesized nanomagnetic CaO-based catalyst, KF/CaO-Fe$_3$O$_4$, was prepared.

2.4. Additives

The heterogeneous CaO-based catalysts with lithium (Li) [22,23] or aluminum (Al) [24] additives were prepared as follows:

2.4.1. Lithium Additives (Li)

Calcined metal oxides (CaO; 100.0 g), 5.0 g Fe$_3$O$_4$ magnetic core, and 1.23% Li additives were mixed homogeneously. Then, metal oxides were mixed using aqueous LiNO$_3$ solutions of the appropriate concentration. The mixed slurry was stirred for 2 h and heated to 100 °C for 2 h [23]. Then, to continue with KF impregnation, drying and calcination were performed, as previously mentioned in Section 2.3. As a result, the KF/CaO-Fe$_3$O$_4$-Li nanomagnetic catalyst was synthesized.

2.4.2. Aluminum Additives (Al)

The molar ratio of NaOH, Al, and calcined metal oxides with Fe$_3$O$_4$ magnetic core was fixed at 2:2:3. Firstly, the NaOH solution was prepared by dissolving NaOH into the distilled water and then Al sheet was added into the solution. After that, the mixed slurry of sodium meta-aluminate solution (mixture of Al and NaOH) was stirred for 2 h and then heated to 100 °C for 2 h [24]. Then,

we continued with KF impregnation, drying, and calcination as previously mentioned in Section 2.3. Finally, after the calcination process, the Al additives catalyst, KF/CaO-Fe$_3$O$_4$-Al, was prepared.

2.5. Transesterification Process

The transesterification reaction was carried out in a 40 mL tubular high-pressure reactor (20 MPa) using the subcritical fluid technique and nanomagnetic catalysts. The reaction temperature was fixed at subcritical methanol condition at 220 °C. The molar ratio between methanol and rubber seed oil was 10:1, 25:1, or 40:1. The synthesized nanomagnetic catalyst was used at 1.5, 3.0, or 4.5 wt % oil and the reaction time was 30, 45, or 60 min. After the reaction occurred completely, the catalyst was removed using a permanent magnet. Then, the two liquid phases, methyl ester and glycerol, were separated by separation funnel. We applied these transesterification process procedures to all 3 types of synthesized nanomagnetic catalysts; KF/CaO-Fe$_3$O$_4$, KF/CaO-Fe$_3$O$_4$-Li, and KF/CaO-Fe$_3$O$_4$-Al.

2.6. Experimental Design and Optimization

The three independent variables, the molar ratio between methanol and rubber seed oil, catalysts amount, and reaction time of rubber seed oil biodiesel production using subcritical methanol with various types of catalysts, were chosen for further optimization studies using RSM. These three variables were chosen because their effects are the most influential in biodiesel production [5,35]. The methanol to rubber seed oil ratio ranged from 10:1 to 40:1, catalysts loading ranged from 1.5 to 4.5 wt %, and reaction time ranged from 30 to 60 min [35,39–41].

A total of 15 runs of Box-Behnken Design (BBD) [36,38,42–44] with three variables at three levels were used in this study. The three levels of each variable examined were coded as –1 for the lower level, 0 for the middle level, and 1 for the higher level, as shown in Table 1. The molar ratio between methanol and rubber seed oil (the individual parameter) was defined as X_1, whereas the amount of catalysts and reaction time in subcritical condition were defined as X_2 and X_3, respectively. The response of each experiment was modeled as a second-order polynomial:

$$Y = \beta_0 + \beta_1 X_1 + \beta_2 X_2 + \beta_3 X_3 + \beta_{11} X_1{}^2 + \beta_{22} X_2{}^2 + \beta_{33} X_3{}^2 + \beta_{12} X_1 X_2 + \beta_{13} X_1 X_3 + \beta_{23} X_2 X_3 \quad (1)$$

where Y is the corresponding response variable and β_i (i = 0, 1, 2, 3, 11, 12, 13, 22, 23, and 33) is the series of regression coefficients for the intercept, linearity, square, and interaction. The independent variables coded are of X_n (n = 1, 2, 3). The experimental design, data analysis, and response surface graphs were calculated and generated by combining regression and graphical analyses. The optimum operating conditions of rubber seed biodiesel production were determined by solving the regression equation and applying RSM. Design Expert Software (Version 11, Stat-Ease, Inc., Minneapolis, MN, USA) was used for data analyzation.

Table 1. The levels of independent variables examined and the range of dependent responses of the rubber seed oil biodiesel production using Box-Behnken design. RSO: Rubber seed oil.

Variable	Coded Level		
	−1	0	1
Molar ratio (X_1, methanol:RSO)	10:1	25:1	40:1
Amount of catalysts (X_2, wt %)	1.5	3	4.5
Reaction time in subcritical condition (X_3, min)	30	45	60

2.7. FAME Analytical Method

The FAME yield percentages were analyzed using gas chromatography (GC; Clarus 680 GC, PerkinElmer Inc., Waltham, MA, USA) with a Perkin Elmer Elite Series GC Column (PE-5 Phase, 60 mm × 0.250 mm, d_f = 0.25 μm) using the European Standard (EN) 14103 (European Standard) method.

The EN 14103 method specifies quality criteria for the biodiesel production via FAME content. The FAME yield from each experiment was calculated from its content in the composition as analyzed by GC.

2.8. Nanomagnetic Catalysts Characterization

The morphology of nanomagnetic CaO-based catalysts were analyzed using scanning electron microscopy (SEM, model JSM-6610LV, JEOL Ltd., Tokyo, Japan). The specific surface area, pore volume, and pore size were measured by nitrogen adsorption-desorption isotherms using a Brunauer-Emmett-Teller (BET) Model Autosorb-1 (Quantachrome Corporation, Boynton Beach, FL, USA).

3. Results and Discussion

3.1. Nanomagnetic Catalysts Properties

The morphologies of CaO powder and nanomagnetic CaO-based catalysts, $KF/CaO-Fe_3O_4$, $KF/CaO-Fe_3O_4$-Li, and $KF/CaO-Fe_3O_4$-Al, are shown in Figure 1a–d, respectively. The SEM images illustrate that nanomagnetic CaO-based catalysts particles were mostly agglomerated and formed into a larger crystal structure, especially $KF/CaO-Fe_3O_4$-Li, with Li additives. $KF/CaO-Fe_3O_4$ catalyst particles also agglomerated, but the overall crystal size was smaller than the Li additives catalysts. Although $KF/CaO-Fe_3O_4$-Al catalysts agglomerated, all small particles were identified.
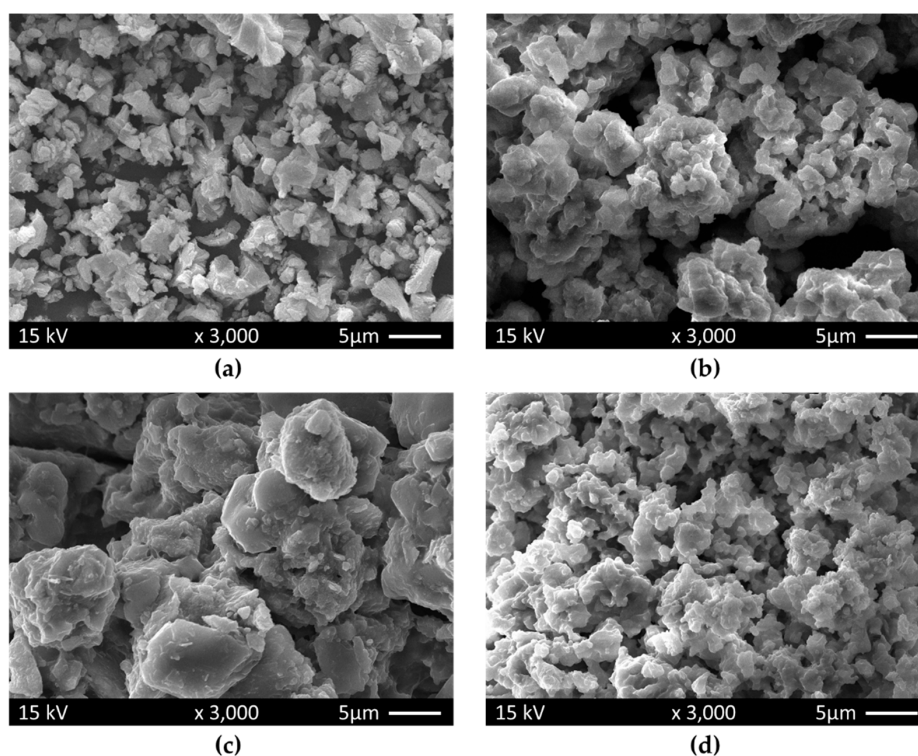

Figure 1. The morphologies of CaO powder and various synthesized nanomagnetic CaO-based catalysts were analyzed using scanning electron microscopy (SEM): (**a**) CaO powder, (**b**) $KF/CaO-Fe_3O_4$, (**c**) $KF/CaO-Fe_3O_4$-Li, and (**d**) $KF/CaO-Fe_3O_4$-Al.

The BET specific surface area, pore volume, and Barrett-Joyner-Halenda (BJH) pore size of CaO powder and synthesized nanomagnetic CaO-based catalysts, $KF/CaO-Fe_3O_4$, $KF/CaO-Fe_3O_4$-Li and $KF/CaO-Fe_3O_4$-Al, are shown in Table 2. The properties of synthesized catalysts dramatically decreased compared to CaO powder due to magnetization and impregnation, due to the pore blockage caused by additives [45]. The specific surface area of synthesized nanomagnetic CaO-based catalyst was 27.84 m^2/g. The surface area increased to 34.93 and 95.70 m^2/g in the presence of Li and Al

additives, respectively. The morphology of Al additive catalysts (Figure 1d) confirm that without the agglomeration effect, small particles were distributed independently, producing a higher specific surface area [46]. The larger surface area of the catalyst provided a larger area for adsorption on the surface, which enhanced the forward reaction [47] and resulted in higher FAME conversion. The pore sizes of the three types of synthesized nanomagnetic CaO-based catalyst ranged from 2.15 to 3.79 nm, which means that mesopores catalysts were produced [45]. The BET results illustrate that the Li additive catalysts had higher selectivity due to their smaller pore size and smaller pore volume compared to the other two synthesized catalysts. In contrast, the Al additive catalysts had the highest surface area, pore volume, and pore size, which led to better catalyst performance [46].

Table 2. Brunauer-Emmett-Teller (BET) specific surface area, pore volume and pore size data of synthesized nanomagnetic catalysts.

Nanomagnetic Catalyst	BET Surface Area (m^2/g)	Pore Volume (cm^3/g)	BJH Pore Size (nm)
CaO	121.00	0.1351	3.79
$KF/CaO-Fe_3O_4$	27.84	0.0510	2.16
$KF/CaO-Fe_3O_4$-Li	34.93	0.0308	2.15
$KF/CaO-Fe_3O_4$-Al	95.70	0.1140	3.79

3.2. Response Surface Methodology Analysis

A Box–Behnken design containing 15 trials was used as the experimental design. Table 3 summarizes the details of the experimental matrix and the corresponding results. The experimental FAME yield data that were analyzed from the rubber seed biodiesels using GC were used to calculate the coefficients of a second-order polynomial:

$$Y = 81.1533 + 7.6263X_1 - 6.3088X_2 - 6.1150X_3 - 11.1054X_1{}^2 - 1.6054X_2{}^2 - 8.2629X_3{}^2 + 3.7425X_1X_2 - 0.0550X_1X_3 - 10.5550X_2X_3 \qquad (2)$$

where Y denotes the predicted FAME yield of rubber seed biodiesel production, and X_1, X_2, and X_3 denote the molar ratio between methanol and rubber seed oil (methanol: RSO), $KF/CaO-Fe_3O_4$-Al catalysts amount (wt %), and reaction time (min), respectively.

Table 3. Box-Behnken design conditions for optimizing the rubber seed oil biodiesel production with corresponding experimental results and predicted response values.

Variables	Molar Ratio		Catalyst Amount		Time		FAME Yield	
(unit)	(methanol:RSO)		(wt %)		(min)		(%)	
Run	X_1	x_1	X_2	x_2	X_3	x_3	Experimental	Predicted
1	10:1	−1	1.5	−1	45	0	72.11	70.87
2	40:1	1	1.5	−1	45	0	78.51	78.64
3	10:1	−1	4.5	1	45	0	50.89	50.77
4	40:1	1	4.5	1	45	0	72.26	73.50
5	10:1	−1	3.0	0	30	−1	60.54	60.22
6	40:1	1	3.0	0	30	−1	77.27	75.58
7	10:1	−1	3.0	0	60	1	46.41	48.10
8	40:1	1	3.0	0	60	1	62.92	63.24
9	25:1	0	1.5	−1	30	−1	71.59	73.15
10	25:1	0	4.5	1	30	−1	81.20	81.65
11	25:1	0	1.5	−1	60	1	82.48	82.03
12	25:1	0	4.5	1	60	1	49.87	48.31
13	25:1	0	3.0	0	45	0	83.32	81.15
14	25:1	0	3.0	0	45	0	81.01	81.15
15	25:1	0	3.0	0	45	0	79.13	81.15

Based on Equation (2), the predicted FAME yield of rubber seed biodiesel is shown in Table 3. The coefficient of determination (R^2) between the experimental and predicted values was determined to be 0.9898, indicating that approximately 98.98% of the variations for the response could be explained. The Analysis of Variance (ANOVA) summary of the RSM is presented in Table 4. The *p*-value of the model term was found to be significant at less than 0.05 as shown in Table 4.

Table 4. ANOVA for quadratic model of the rubber seed oil biodiesel production. D_f: Degrees of freedom; pred R^2: Predicted value of R-squared; adj R^2: Adjusted R-squared; adeq: Adequacy of R-squared.

Source	Sum of Squares	D_f	Mean Square	F-Value	*p*-Value Probability > F
Model	2243.92	9	249.32	53.90	0.0002
X_1	465.28	1	465.28	100.59	0.0002
X_2	318.40	1	318.40	68.84	0.0004
X_3	299.15	1	299.15	64.68	0.0005
X_1X_2	56.03	1	56.03	12.11	0.0177
X_1X_3	0.01	1	0.01	0.00	0.9612
X_2X_3	445.63	1	445.63	96.35	0.0002
$X_1{}^2$	455.37	1	455.37	98.45	0.0002
$X_2{}^2$	9.52	1	9.52	2.06	0.2109
$X_3{}^2$	252.10	1	252.10	54.50	0.0007
Residual	23.13	5	4.63		
Lack of fit	14.32	3	4.77	1.08	0.5129
Pure error	8.81	2	4.40		
SD	R^2	pred R^2	adj R^2	adeq precision	Mean
2.15	0.9898	0.8902	0.9714	19.3251	69.97

The response surface curves and contour plots of three independent variables illustrated in Figures 2–4 were generated based on the regression model. Both the influence and interaction of each independent variable were evaluated. Each of the response surfaces, as shown in Figures 2–4, produced a clear peak point that indicated that optimum condition and the maximum FAME yield in rubber seed biodiesel production, which were achieved inside the design boundary region for all three variables. The optimum values of X_1, X_2, and X_3 derived from Equation (2) were −0.1749, −0.7829 and 0.3974, respectively. Hence, the optimum point of the model includes a 28:1 molar ratio between methanol and RSO, 1.5 wt % of KF/CaO-Fe$_3$O$_4$-Al catalyst, and a 49 min reaction time. The optimum condition leads to the maximum predicted value of FAME yield of 86.79%.
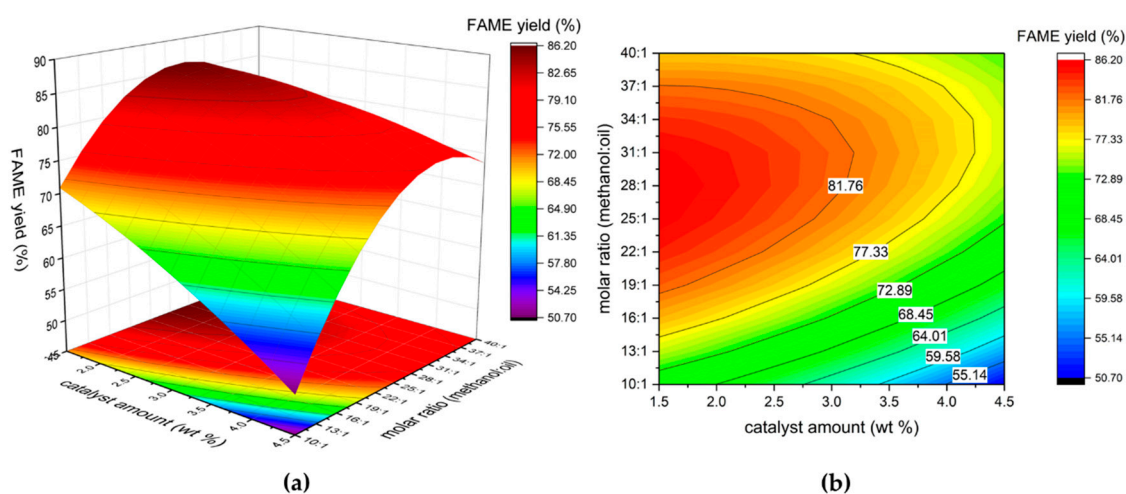

Figure 2. The interaction effect of molar ratio and KF/CaO-Fe$_3$O$_4$-Al catalyst amount on FAME yield for rubber seed biodiesel production: (**a**) response surface curve and (**b**) contour plot.
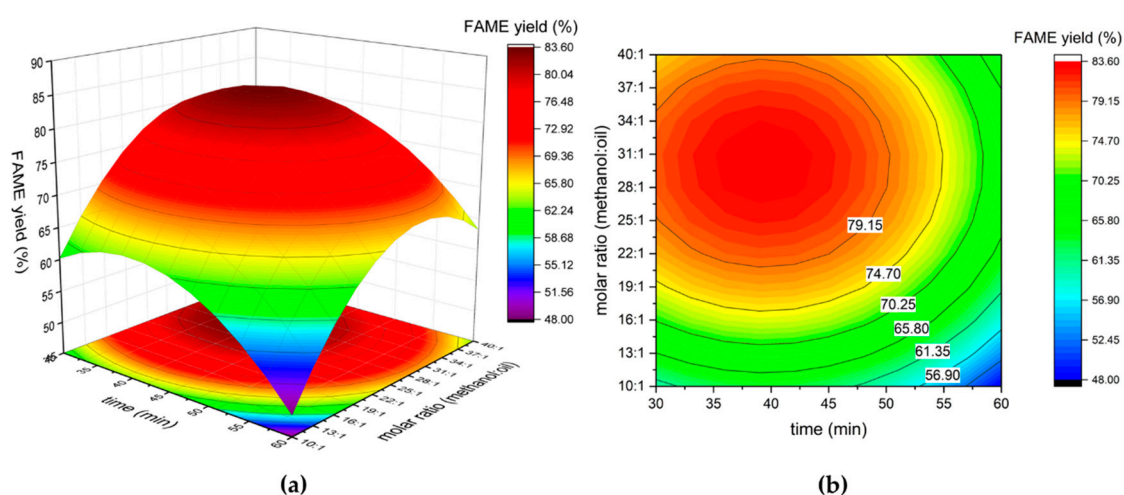
Figure 3. The interaction effect of molar ratio and reaction time on FAME yield for rubber seed biodiesel production: (**a**) response surface curve and (**b**) contour plot.
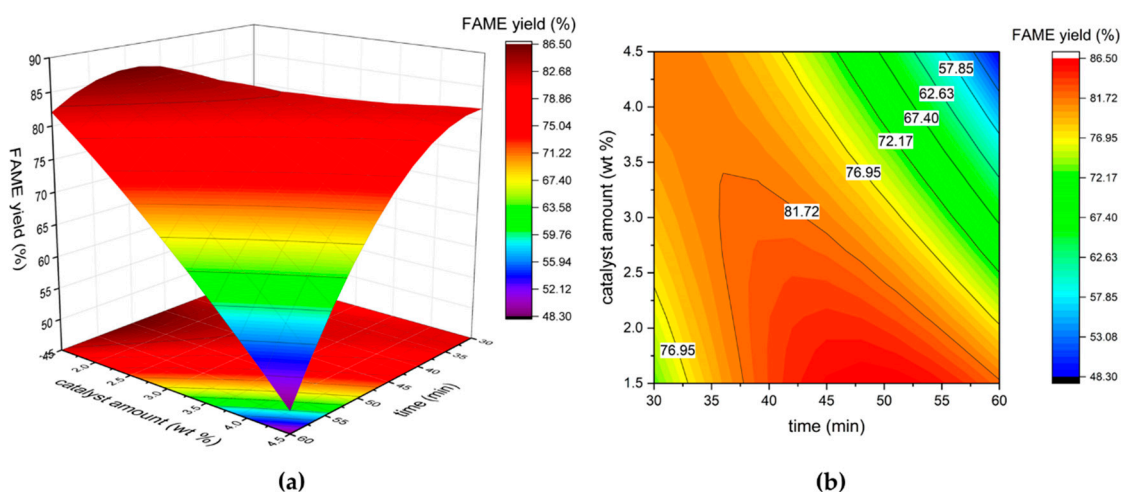

Figure 4. The interaction effect of KF/CaO-Fe$_3$O$_4$-Al catalyst amount and reaction time on FAME yield for rubber seed biodiesel production: (**a**) response surface curve and (**b**) contour plot.

The response surface illustrated in Figure 2 represents the interaction effect of molar ratio (X_1) from 10:1 to 40:1 and KF/CaO-Fe$_3$O$_4$-Al catalyst amount (X_2) from 1.5 to 4.5 wt % at a constant reaction time (X_3) of 45 min. It can be observed that the highest FAME yield percentage was produced at a 28:1 molar ratio and 1.5 wt % catalyst. As the molar ratio increased, the FAME yield increased [30]. The FAME yield continuously increased by introducing more methanol to shift the equilibrium to the right-hand side, but when the ratio was more than 37:1, then the excess methanol would cause the FAME yield to decrease. The low level of excess methanol in biodiesel production encourages the RSO to FAME conversion, but at some point (in this work, at 37:1) the excess methanol and rubber seed oil separated into two phases of fluids, which caused a shift in the biodiesel conversion step [48,49]. A high molar ratio of methanol to oil increased FAME conversion, which confirmed the data in Table 3 for runs 2 and 3. The contour in Figure 2 shows that a lower catalysts usage enhances FAME yield percentage. This was caused by excess catalysts remaining in the system, which resulted in lower FAME conversion [48]. In additional, excess catalyst caused lower FAME percentages, confirmed by the data in Table 3 for runs 11 and 12.

The response surface shown in Figure 3 represents the interaction effect of molar ratio (X_1) in the range of 10:1 to 40:1 and reaction time (X_3) from 30 to 60 min at constant KF/CaO-Fe$_3$O$_4$-Al catalyst amount (X_2) of 3 wt %. It can be observed that the highest FAME yield was produced by an approximately 30:1 molar ratio and 38 min reaction time. The FAME yield increased due to the

increasing molar ratio. Similar to the previous paragraph, the FAME yield increased by introducing more methanol but with excess methanol, the FAME yield began to decrease [48,49]. The response surface also indicates that the advantage of subcritical methanol for biodiesel production is that it significantly reduces the reaction time compared to the KOH conventional method for biodiesel production, which requires more than 120 min to complete the process [50].

The response surface illustrated in Figure 4 represents the interaction effect when the KF/CaO-Fe$_3$O$_4$-Al catalyst amount (X_2) was varied from 1.5 to 3 wt % and reaction time (X_3) was increased from 30 to 60 min at a constant molar ratio (X_1) of 25:1. It can be observed that the highest FAME yield percentage was produced at 1.5 wt % of catalyst and 47 min reaction time. Similar to Figure 2, the amount of remaining excess catalysts led to lower FAME conversion due to rubber seed oil separating into two liquid phases, causing a shift in the biodiesel conversion step [48]. Using a small amount of catalysts is recommended. In general, the high FFA content in the feedstock oil should be esterified and run through two-step biodiesel production, which is time consuming and complicated [50]. In this work, subcritical methanol successfully produced biodiesel with the single-step transesterification of a high-FFA feedstock, rubber seed oil. The contour in Figure 4 shows that the FAME yield peaked at approximately 48 min of reaction time.

3.3. Comparison of Nanomagnetic Catalysts and Subcritical Methanol Performance

The optimum condition of three types of nanomagnetic catalysts, KF/CaO-Fe$_3$O$_4$, KF/CaO-Fe$_3$O$_4$-Li and KF/CaO-Fe$_3$O$_4$-Al for rubber seed biodiesel production were investigated in this work. The role of different components in various catalysts produces different FAME yields. Overall, the nanomagnetic CaO-based catalyst with additives appeared to perform better and produced higher FAME yields than the one without additives. The Li additives affected the transesterification in biodiesel production [22,23,51,52]. A high free fatty acids (FFA) content in RSO [7,10,53,54] significantly affected the catalysts performance compared to the other types of oil [16,23,24].

The roles of different types and components in nanomagnetic CaO-based catalysts were investigated through the optimum conditions and FAME yield of rubber seed biodiesel production, shown in Table 5. Overall, the synthesized catalysts significantly reduced the catalyst amount and reaction time required for biodiesel production and show the reasonable FAME yield as mentioned in the previous paragraph. In rubber seed biodiesel production, limestone-based catalysts produce a higher FAME yield [55], but the process is time consuming (by approximately more than four times) compared to the catalysts synthesized in this work. Limestone-based catalysts are complicated to prepare and have variable compositions such as Cao, SiO$_2$, Al$_2$O$_3$, Fe$_2$O$_3$, MgO, SO$_3$, K$_2$O, Na$_2$O, P$_2$O$_5$, and TiO$_2$ [55]. The acceptable FAME yield was determined to be 80%, and a high FAME yield is considered to be 85%. Hence, the FAME yield of KF/CaO-Fe$_3$O$_4$-Li is acceptable and the FAME yield for KF/CaO-Fe$_3$O$_4$-Al is considered high. The results indicate that both Li and Al additives significantly improved catalyst performance (from KF/CaO-Fe$_3$O$_4$). The reaction of alkali catalyst in Li additives or sodium meta-aluminate in Al additives catalysts with free fatty acids reduced saponification and enhanced methyl esters formation [22–24].

Various types of CaO-based catalyst are commonly used in *Jatropha curcas* biodiesel production. *Jatropha curcas* oil has a high FFA content (14–15%), which is similar to that of rubber seed oil [56–58]. The results showed that the nanomagnetic CaO-based catalysts synthesized in this work have better performance due to their faster reaction time, lower catalyst amount required, and easier removal with a permanent magnet [19–21]. Table 5 illustrated that Al-additive catalysts produced a yield of 86.79%, which was the highest FAME yield in this work and is competitive compared to other catalysts previously analyzed in the literature. The time required for biodiesel production using these catalysts was much shorter and used significantly less catalyst. Besides catalysts performance, the major advantages of all three types of synthesized nanomagnetic CaO-based catalysts are that they are easily removed after reaction and the produced biodiesel was clearly separated from the glycerol, which enhanced FAME yield.

Table 5. Comparison of optimum conditions with various catalysts for biodiesel production achieved during this work and other works.

Type of Catalyst	Biodiesel Source	Optimum Conditions				Reference
		Molar Ratio (Methanol:RSO)	Catalyst Amount (wt %)	Time (min)	FAME Yield (%)	
KF/CaO-Fe$_3$O$_4$	Rubber seed oil	34:1	1.6	60	68.62	This work
KF/CaO-Fe$_3$O$_4$-Li	Rubber seed oil	26:1	1.5	60	84.86	This work
KF/CaO-Fe$_3$O$_4$-Al	Rubber seed oil	28:1	1.5	49	86.79	This work
KF/CaO-Fe$_3$O$_4$	*Stillingia* oil	12:1	4	180	95.0	[16]
Limestone based (CaO, SiO$_2$, Al$_2$O$_3$, Fe$_2$O$_3$, MgO, SO$_3$, K$_2$O, Na$_2$O, P$_2$O$_5$ and TiO$_2$)	Rubber seed oil	5:1	5	240	96.9	[55]
CaO/Li	Karanja oil	12:1	2	480	94.9	[23]
CaMgO	*Jatropha curcas*	15:1	4	360	83	[19]
CaZnO	*Jatropha curcas*	15:1	4	360	81	[19]
CaO-NiO	*Jatropha curcas*	15:1	5	360	86.3	[20]
CaO-Nd$_2$O$_3$	*Jatropha curcas*	15:1	5	360	82.2	[20]
CaO-La$_2$O$_3$	*Jatropha curcas*	24:1	4	360	86.5	[21]
CaO/Al/Fe$_3$O$_4$	Rapeseed oil	15:1	6	180	98.71	[24]

4. Conclusions

Rubber seeds are agricultural residuals that have potential for use as a non-edible biodiesel raw material. Rubber seed oil successfully produced biodiesel through the transesterification process using subcritical methanol with nanomagnetic catalysts: KF/CaO-Fe$_3$O$_4$, KF/CaO-Fe$_3$O$_4$-Li, and KF/CaO-Fe$_3$O$_4$-Al. Response surface methodology with the Box-Behnken design was employed to determine a feasible experimental plan to optimize the rubber seed oil for the biodiesel conversion procedure due to the high FFA content of RSO (16.7%). The effect of all three independent parameters (methanol to oil molar ratio of 10:1–40:1, catalysts loading of 1.5–4.5 wt %, and reaction time of 30–60 min) were statistically investigated on the fatty acid methyl ester yield for rubber seed biodiesel production at 220 °C. The limitation of the developed response surface model is that all the *p*-values were less than 0.05. KF/CaO-Fe$_3$O$_4$-Al is nanomagnetic catalyst with a BET surface area of 95.70 m^2/g, pore volume of 0.1140 cm3/g, BJH pore size of 3.79 nm, and the highest FAME yield. The optimal conditions for Al additives of KF/CaO-Fe$_3$O$_4$ nanomagnetic catalyst enhanced FAME yield without Al up to 18.17% and the process was 11 min faster, while Li additives enhanced FAME yield without Li up to 16.24%. The optimum conditions for rubber seed biodiesel production using the subcritical methanol with KF/CaO-Fe$_3$O$_4$-Al as the nanomagnetic catalyst were optimized as a 28:1 molar ratio of methanol to RSO, 1.5 wt % catalyst, and 49 min reaction time. The optimum conditions led to the maximum predicted FAME yield of 86.79%.

References

1. Martchamadol, J.; Kumar, S. Thailand's energy security indicators. *Renew. Sustain. Energy Rev.* **2012**, *16*, 6103–6122. [CrossRef]
2. Abas, N.; Kalair, A.; Khan, N. Review of fossil fuels and future energy technologies. *Futures* **2015**, *69*, 31–49. [CrossRef]

3. Refaat, A.A. Biodiesel production using solid metal oxide catalysts. *Int. J. Environ. Sci. Technol.* **2011**, *8*, 203–221. [CrossRef]

4. Siriwardhana, M.; Opathella, G.K.C.; Jha, M.K. Bio-diesel: Initiatives, potential and prospects in Thailand: A review. *Energy Policy* **2009**, *37*, 554–559. [CrossRef]

5. Takase, M.; Zhao, T.; Zhang, M.; Chen, Y.; Liu, H.; Yang, L.; Wu, X. An expatiate review of neem, jatropha, rubber and karanja as multipurpose non-edible biodiesel resources and comparison of their fuel, engine and emission properties. *Renew. Sustain. Energy Rev.* **2015**, *43*, 495–520. [CrossRef]

6. Alengaram, U.J.; Al Muhit, B.A.; bin Jumaat, M.Z. Utilization of oil palm kernel shell as lightweight aggregate in concrete—A review. *Constr. Build. Mater.* **2013**, *38*, 161–172. [CrossRef]

7. Samart, C.; Karnjanakom, S.; Chaiya, C.; Reubroycharoen, P.; Sawangkeaw, R.; Charoenpanich, M. Statistical optimization of biodiesel production from para rubber seed oil by SO_3H-MCM-41 catalyst. *Arabian J. Chem.* **2015**. [CrossRef]

8. Gimbun, J.; Ali, S.; Kanwal, C.C.S.C.; Shah, L.A.; Muhamad, N.H.; Cheng, C.K.; Nurdin, S. Biodiesel Production from Rubber Seed Oil using Activated Cement Clinker as Catalyst. *Procedia Eng.* **2013**, *53*, 13–19. [CrossRef]

9. Wibowo, A.D.K. Study on Production Process of Biodiesel from Rubber Seed (*Hevea Brasiliensis*) by in Situ (Trans)Esterification Method with Acid Catalyst. *Energy Procedia* **2013**, *32*, 64–73.

10. Morshed, M.; Ferdous, K.; Khan, M.R.; Mazumder, M.S.I.; Islam, M.A.; Uddin, M.T. Rubber seed oil as a potential source for biodiesel production in Bangladesh. *Fuel* **2011**, *90*, 2981–2986. [CrossRef]

11. Mukherjee, I.; Sovacool, B.K. Palm oil-based biofuels and sustainability in southeast Asia: A review of Indonesia, Malaysia, and Thailand. *Renew. Sustain. Energy Rev.* **2014**, *37*, 1–12. [CrossRef]

12. Ahmad, J.; Yusup, S.; Bokhari, A.; Kamil, R.N.M. Study of fuel properties of rubber seed oil based biodiesel. *Energy Conver. Manag.* **2014**, *78*, 266–275. [CrossRef]

13. Roschat, W.; Siritanon, T.; Yoosuk, B.; Sudyoadsuk, T.; Promarak, V. Rubber seed oil as potential non-edible feedstock for biodiesel production using heterogeneous catalyst in Thailand. *Renew. Energy* **2017**, *101*, 937–944. [CrossRef]

14. Liu, H.; Su, L.; Shao, Y.; Zou, L. Biodiesel production catalyzed by cinder supported CaO/KF particle catalyst. *Fuel* **2012**, *97*, 651–657. [CrossRef]

15. Reshad, A.S.; Tiwari, P.; Goud, V.V. Extraction of oil from rubber seeds for biodiesel application: Optimization of parameters. *Fuel* **2015**, *150*, 636–644. [CrossRef]

16. Hu, S.; Guan, Y.; Wang, Y.; Han, H. Nano-magnetic catalyst KF/CaO–Fe_3O_4 for biodiesel production. *Applied Energy* **2011**, *88*, 2685–2690. [CrossRef]

17. Bet-Moushoul, E.; Farhadi, K.; Mansourpanah, Y.; Nikbakht, A.M.; Molaei, R.; Forough, M. Application of CaO-based/Au nanoparticles as heterogeneous nanocatalysts in biodiesel production. *Fuel* **2016**, *164*, 119–127. [CrossRef]

18. Marwaha, A.; Rosha, P.; Mohapatra, S.K.; Mahla, S.K.; Dhir, A. Waste materials as potential catalysts for biodiesel production: Current state and future scope. *Fuel Process. Technol.* **2018**, *181*, 175–186. [CrossRef]

19. Taufiq-Yap, Y.H.; Lee, H.V.; Hussein, M.Z.; Yunus, R. Calcium-based mixed oxide catalysts for methanolysis of *Jatropha curcas* oil to biodiesel. *Biomass Bioenergy* **2011**, *35*, 827–834. [CrossRef]

20. Teo, S.H.; Rashid, U.; Taufiq-Yap, Y.H. Biodiesel production from crude *Jatropha Curcas* oil using calcium based mixed oxide catalysts. *Fuel* **2014**, *136*, 244–252. [CrossRef]

21. Taufiq-Yap, Y.H.; Teo, S.H.; Rashid, U.; Islam, A.; Hussien, M.Z.; Lee, K.T. Transesterification of *Jatropha curcas* crude oil to biodiesel on calcium lanthanum mixed oxide catalyst: Effect of stoichiometric composition. *Energy Convers. Manag.* **2014**, *88*, 1290–1296. [CrossRef]

22. MacLeod, C.S.; Harvey, A.P.; Lee, A.F.; Wilson, K. Evaluation of the activity and stability of alkali-doped metal oxide catalysts for application to an intensified method of biodiesel production. *Chem. Eng. J.* **2008**, *135*, 63–70. [CrossRef]

23. Meher, L.C.; Dharmagadda, V.S.S.; Naik, S.N. Optimization of alkali-catalyzed transesterification of *Pongamia pinnata* oil for production of biodiesel. *Bioresour. Technol.* **2006**, *97*, 1392–1397. [CrossRef] [PubMed]

24. Tang, S.; Wang, L.; Zhang, Y.; Li, S.; Tian, S.; Wang, B. Study on preparation of Ca/Al/Fe_3O_4 magnetic composite solid catalyst and its application in biodiesel transesterification. *Fuel Process. Technol.* **2012**, *95*, 84–89. [CrossRef]

25. Xie, W.; Peng, H.; Chen, L. Calcined Mg-Al hydrotalcites as solid base catalysts for methanolysis of soybean oil. *J. Mol. Catal. A Chem.* **2006**, *246*, 24–32. [CrossRef]

26. Sitthithanaboon, W.; Reddy, H.K.; Muppaneni, T.; Ponnusamy, S.; Punsuvon, V.; Holguim, F.; Dungan, B.; Deng, S. Single-step conversion of wet *Nannochloropsis gaditana* to biodiesel under subcritical methanol conditions. *Fuel* **2015**, *147*, 253–259. [CrossRef]

27. Micic, R.D.; Tomić, M.D.; Kiss, F.E.; Nikolić-Djorić, E.B.; Simikić, M.Đ. Optimization of hydrolysis in subcritical water as a pretreatment step for biodiesel production by esterification in supercritical methanol. *J. Supercrit. Fluids* **2015**, *103*, 90–100. [CrossRef]

28. Yin, J.-Z.; Ma, Z.; Shang, Z.-Y.; Hu, D.-P.; Xiu, Z.-L. Biodiesel production from soybean oil transesterification in subcritical methanol with K_3PO_4 as a catalyst. *Fuel* **2012**, *93*, 284–287. [CrossRef]

29. Sánchez, N.; Encinar, J.M.; Martínez, G.; González, J.F. Biodiesel Production from Castor Oil under Subcritical Methanol Conditions. *Int. J. Environ. Sci. Dev.* **2015**, *6*, 61.

30. Yin, J.-Z.; Ma, Z.; Hu, D.-P.; Xiu, Z.-L.; Wang, T.-H. Biodiesel Production from Subcritical Methanol Transesterification of Soybean Oil with Sodium Silicate. *Energy Fuels* **2010**, *24*, 3179–3182. [CrossRef]

31. Edem, D.O. Palm oil: Biochemical, physiological, nutritional, hematological and toxicological aspects: A review. *Plant Foods Hum. Nutr.* **2002**, *57*, 319–341. [CrossRef] [PubMed]

32. Jahirul, M.I.; Koh, W.; Brown, R.J.; Senadeera, W.; O'Hara, I.; Moghaddam, L. Biodiesel Production from Non-Edible Beauty Leaf (*Calophyllum inophyllum*) Oil: Process Optimization Using Response Surface Methodology (RSM). *Energies* **2014**, *7*, 5317–5331. [CrossRef]

33. Onumaegbu, C.; Alaswad, A.; Rodriguez, C.; Olabi, A.G. Optimization of Pre-Treatment Process Parameters to Generate Biodiesel from Microalga. *Energies* **2018**, *11*, 806. [CrossRef]

34. Bobadilla, M.C.; Martínez, R.F.; Lorza, R.L.; Gómez, F.S.; González, E.P.V. Optimizing Biodiesel Production from Waste Cooking Oil Using Genetic Algorithm-Based Support Vector Machines. *Energies* **2018**, *11*, 2995. [CrossRef]

35. Onoji, S.E.; Iyuke, S.E.; Igbafe, A.I.; Daramola, M.O. Transesterification of Rubber Seed Oil to Biodiesel over a Calcined Waste Rubber Seed Shell Catalyst: Modeling and Optimization of Process Variables. *Energy Fuels* **2017**, *31*, 6109–6119. [CrossRef]

36. Betiku, E.; Etim, A.O.; Pereao, O.; Ojumu, T.V. Two-Step Conversion of Neem (*Azadirachta indica*) Seed Oil into Fatty Methyl Esters Using a Heterogeneous Biomass-Based Catalyst: An Example of Cocoa Pod Husk. *Energy Fuels* **2017**, *31*, 6182–6193. [CrossRef]

37. Das, D.; Thakur, R.; Pradhan, A.K. Optimization of corona discharge process using Box–Behnken design of experiments. *J. Electrostat.* **2012**, *70*, 469–473. [CrossRef]

38. Yin, Y.; Wang, J. Optimization of Hydrogen Production by Response Surface Methodology Using γ-Irradiated Sludge as Inoculum. *Energy Fuels* **2016**, *30*, 4096–4103. [CrossRef]

39. Hebbar, H.R.H.; Math, M.C.; Yatish, K.V. Optimization and kinetic study of CaO nano-particles catalyzed biodiesel production from Bombax ceiba oil. *Energy* **2018**, *143*, 25–34. [CrossRef]

40. Khazaai, S.N.M.; Maniam, G.P.; Rahim, M.H.A.; Yusoff, M.M.; Matsumura, Y. Review on methyl ester production from inedible rubber seed oil under various catalysts. *Ind. Crop. Prod.* **2017**, *97*, 191–195. [CrossRef]

41. Mansir, N.; Teo, S.H.; Rashid, U.; Taufiq-Yap, Y.H. Efficient waste *Gallus domesticus* shell derived calcium-based catalyst for biodiesel production. *Fuel* **2018**, *211*, 67–75. [CrossRef]

42. Box, G.E.P.; Behnken, D.W. Some New Three Level Designs for the Study of Quantitative Variables. *Technometrics* **1960**, *2*, 455–475. [CrossRef]

43. Wu, Z.; Chen, C.; Wan, H.; Wang, L.; Li, Z.; Li, B.; Guo, Q.; Guan, G. Fabrication of Magnetic NH_2-MIL-88B (Fe) Confined Brønsted Ionic Liquid as an Efficient Catalyst in Biodiesel Synthesis. *Energy Fuels* **2016**, *30*, 10739–10746. [CrossRef]

44. Zhang, J.; Sun, H.; Pan, C.; Fan, Y.; Hou, H. Optimization of Process Parameters for Directly Converting Raw Corn Stalk to Biohydrogen by *Clostridium* sp. FZ11 without Substrate Pretreatment. *Energy Fuels* **2015**, *30*, 311–317. [CrossRef]

45. Rezayan, A.; Taghizadeh, M. Synthesis of magnetic mesoporous nanocrystalline KOH/ZSM-5-Fe_3O_4 for biodiesel production: Process optimization and kinetics study. *Process Saf. Environ. Protect.* **2018**, *117*, 711–721. [CrossRef]

46. Atadashi, I.M.; Aroua, M.K.; Aziz, A.R.A.; Sulaiman, N.M.N. The effects of catalysts in biodiesel production: A review. *J. Ind. Eng. Chem.* **2013**, *19*, 14–26. [CrossRef]

47. Levenspiel, O. Chemical Reaction Engineering. *Ind. Eng. Chem. Res.* **1999**, *38*, 4140–4143. [CrossRef]

48. Encinar, J.M.; Pardal, A.; Martinez, G. Transesterification of rapeseed oil in subcritical methanol conditions. *Fuel Process. Technol.* **2012**, *94*, 40–46. [CrossRef]

49. Go, A.W.; Nguyen, P.L.T.; Huynh, L.H.; Liu, Y.-T.; Sutanto, S.; Ju, Y.-H. Catalyst free esterification of fatty acids with methanol under subcritical condition. *Energy* **2014**, *70*, 393–400. [CrossRef]

50. Patil, P.D.; Gude, V.G.; Deng, S. Transesterification of *Camelina Sativa* Oil using Supercritical and Subcritical Methanol with Cosolvents. *Energy Fuels* **2009**, *24*, 746–751. [CrossRef]

51. Alonso, D.M.; Mariscal, R.; Granados, M.L.; Maireles-Torres, P. Biodiesel preparation using Li/CaO catalysts: Activation process and homogeneous contribution. *Catal. Today* **2009**, *143*, 167–171. [CrossRef]

52. Kaur, M.; Ali, A. Lithium ion impregnated calcium oxide as nano catalyst for the biodiesel production from karanja and jatropha oils. *Renew. Energy* **2011**, *36*, 2866–2871. [CrossRef]

53. Onoji, S.E.; Iyuke, S.E.; Igbafe, A.I.; Nkazi, D.B. Rubber seed oil: A potential renewable source of biodiesel for sustainable development in sub-Saharan Africa. *Energy Convers. Manag.* **2016**, *110*, 125–134. [CrossRef]

54. Ramadhas, A.S.; Jayaraj, S.; Muraleedharan, C. Biodiesel production from high FFA rubber seed oil. *Fuel* **2005**, *84*, 335–340. [CrossRef]

55. Gimbun, J.; Ali, S.; Kanwal, C.; Shah, L.A.; Ghazali, N.H.M.; Cheng, C.K.; Nurdin, S. Biodiesel Production from Rubber Seed Oil Using A Limestone Based Catalyst. *Adv. Mater. Phys. Chem.* **2012**, *2*, 138–141. [CrossRef]

56. Silitonga, A.S.; Ong, H.C.; Mahlia, T.M.I.; Masjuki, H.H.; Chong, W.T. Biodiesel Conversion from High FFA Crude *Jatropha Curcas*, *Calophyllum Inophyllum* and *Ceiba Pentandra* Oil. *Energy Procedia* **2014**, *61*, 480–483. [CrossRef]

57. Berchmans, H.J.; Hirata, S. Biodiesel production from crude *Jatropha curcas* L. seed oil with a high content of free fatty acids. *Bioresour. Technol.* **2008**, *99*, 1716–1721. [CrossRef]

58. Tiwari, A.K.; Kumar, A.; Raheman, H. Biodiesel production from jatropha oil (*Jatropha curcas*) with high free fatty acids: An optimized process. *Biomass Bioenergy* **2007**, *31*, 569–575. [CrossRef]